European Journal of Medicinal Chemistry 84 (2014) 677–686

Contents lists available at ScienceDirect

European Journal of Medicinal Chemistry

journal homepage: http://www.elsevier.com/locate/ejmech

Original article

The synthesis and activities of novel mononuclear or dinuclear cyclen complexes bearing azole pendants as antibacterial and antifungal agents

Shuo Li [b, *], Jia-Xuan Chen [a], Qing-Xiang Xiang [a, *], Li-Qun Zhang [a], Cheng-He Zhou [c, *], Jia-Qing Xie [b], Lan Yu [b], Fang-Zhen Li [b]

[a] Department of Chemistry, Leshan Normal University, Leshan, Sichuan 614000, People's Republic of China
[b] School of Chemical Engineering, Chongqing University of Technology, Chongqing 400054, People's Republic of China
[c] Laboratory of Bioorganic & Medicinal Chemistry, School of Chemistry and Chemical Engineering, Southwest University, Chongqing 400715, People's Republic of China

ARTICLE INFO

Article history:
Received 7 December 2013
Received in revised form
19 July 2014
Accepted 21 July 2014
Available online 22 July 2014

Keywords:
Azoles
Cyclen
Antibacterial
Antifungal
Fluorescence spectrum

ABSTRACT

A series of novel compounds containing 1,4,7,10-tetraazacyclododecane and azoles were synthesized and characterized by ^{1}H NMR, MS and elemental analysis. Bioactive assay manifested that some target compounds, such as **11a**, **11b** and **11d**, displayed good and broad spectrum antimicrobial activities with relative low MIC values against most of tested strains. These dinuclear complexes gave comparable or even better antimicrobial efficiencies than the reference drugs *Fluconazole* and *Chloromycin*. The result showed that the metal ions were the key factors to enhance the antimicrobial activities for mononuclear or dinuclear complexed in varying degrees. The interaction evaluation of compound **11b** with bovine serum albumin (BSA) as an example was tested by fluorescence method. The thermodynamic parameters indicated that the hydrogen bonds and van der waals forces played the major roles in the strong association between dinuclear compound and BSA. The CCK-8 tests also confirmed the safeties of these dinuclear compounds *in vitro*.

1. Introduction

The increasing emergence of pathogenic bacterial strains and concerns about multidrug-resistance, especially the explosion of New Delhi metallo-β-lactamase 1 (NDM-1) superbugs very recently, had made most of the first-line clinical antibiotics ineffective [1]. This situation has stimulated an urgent need to develop more effective antimicrobial agents with novel chemical structures which are helpful for overcoming drug-resistance and improving the antimicrobial potency.

As we know, heterocyclic compounds such as imidazole, benzimidazole, pyrazole and triazole have been frequently found to display a variety of biological activities such as antihelmintic [2], antihistaminic [3], anticancer [4], antiviral [5], antiinflammatory [6], antiproliferative [7], antioxidant [8], anticoagulant properties [9], antitubercular [10], anticonvulsant [11]. Particularly, many benzimidazole drugs like antiparasitic thiabendazole, mebendazole, albendazole, antihistaminic norastemizole and mizolastine, as well as antihypertensive telmisartan etc. have been successfully developed and extensively used in clinic. This has attracted increasing interest to investigate the possible applications of azole-based derivatives in medicinal aspects. What's more important is that numerous azole supermolecules as chemical drugs are under actively ongoing researches and developments, and have shown enormous potential [12]. It is undoubted that this research area will become a new direction for the exploitation of azole complex as antimicrobial drugs [13], and azole derivatives coordinating with metal cation to form complexes always showed enhanced antimicrobial properties [14]. Besides these azole derivatives, macrocyclic compounds are already extensively exploited for their medical applications as MRI agents [15], antibacterial and anticancer agents [16]. As a well-known macrocyclic polyamine, 1,4,7,10-tetraazacyclododecane (cyclen) has been widely studied for its strong coordination ability towards a wide range of cations, and the safeties of some macrocyclic compounds used *in vivo* have been confirmed. Recently, the increasing prevalence strategy to develope new classes of antimicrobial agents with novel mechanism of

* Corresponding authors.
E-mail addresses: lishuo@cqut.edu.cn, gaoshan210@163.com (S. Li), qxxiang711@163.com (Q.-X. Xiang).

http://dx.doi.org/10.1016/j.ejmech.2014.07.075
0223-5234/

action was to employ combination of two different active fragments into one molecule [17]. So that, in view of above observation, it is reasonable for us with great interest to prepare cyclen complexes having azoles pendants, and to evaluate their antibacterial and antifungal behaviours. Herein a series of novel compounds were prepared for the first time (Schemes 1 and 2). Their antibacterial and antifungal activities were evaluated, and the structure–activity relationships were also investigated.

Serum albumins as the most important and abundant macromolecule proteins in the circulatory system have received much attention for that they could deliver drugs or other bioactive small molecules to the binding sites [18]. A thorough binding analysis between drugs or bioactive small molecules and serum albumin may beneficially provide useful information for the absorption, transportation, distribution, metabolism and excretion properties of drugs. It might also be significant for design, modification and screening of drug molecules. So that there were many important reasons for us to further investigate the interaction behaviour between the highly active compound and bovine serum albumin (BSA) which was used as study model to preliminarily evaluate their transportation and pharmacokinetic properties by fluorescence spectroscopy on molecular level. Further more, the safety or toxicity of those dinuclear complexes were tested by CCK-8 method.

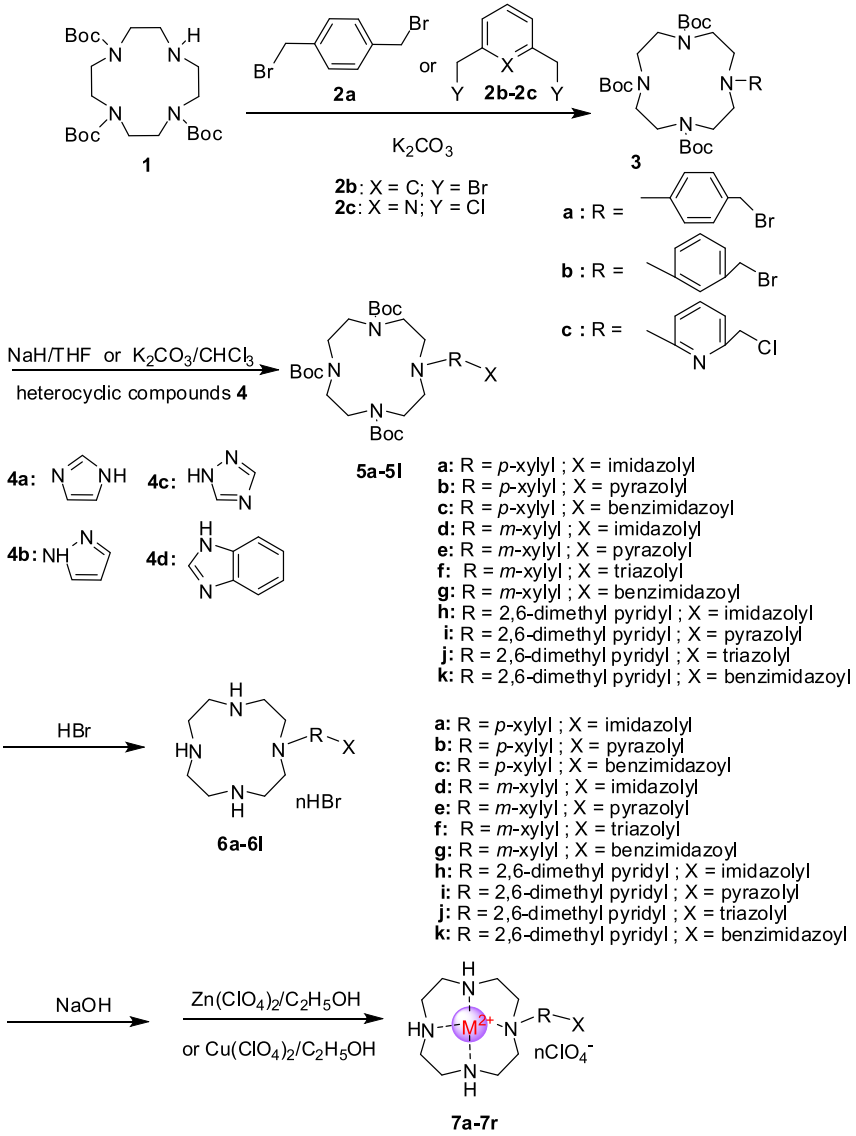

a: R = *p*-xylyl ; X = imidazolyl ; M = Zn; n = 2;
b: R = *p*-xylyl ; X = imidazolyl ; M = Cu; n = 2;
c: R = *p*-xylyl ; X = pyrazolyl ; M = Zn ; n = 2;
d: R = *p*-xylyl ; X = benzimidazoyl ; M = Zn; n = 3;
e: R = *p*-xylyl ; X = benzimidazoyl ; M = Cu; n = 2;
f: R = *m*-xylyl ; X = imidazolyl ; M = Zn; n = 2;
g: R = *m*-xylyl ; X = imidazolyl ; M = Cu; n = 2;
h: R = *m*-xylyl ; X = pyrazolyl ; M = Zn; n = 4;
i: R = *m*-xylyl ; X = pyrazolyl ; M = Cu; n = 2;
j: R = *m*-xylyl ; X = triazolyl ; M = Zn; n = 2;
k: R = *m*-xylyl ; X = benzimidazoyl ; M = Zn; n = 2;
l: R = *m*-xylyl ; X = benzimidazoyl ; M = Cu; n = 2;
m: R = 2,6-dimethyl pyridyl ; X = imidazolyl ; M = Zn; n = 2;
n: R = 2,6-dimethyl pyridyl ; X = pyrazolyl ; M = Zn; n = 2;
o: R = 2,6-dimethyl pyridyl ; X = triazolyl ; M = Zn; n = 3;
p: R = 2,6-dimethyl pyridyl ; X = triazolyl ; M = Cu; n = 3;
q: R = 2,6-dimethyl pyridyl ; X = benzimidazoyl ; M = Zn; n = 3;
r: R = 2,6-dimethyl pyridyl ; X = benzimidazoyl ; M = Cu; n = 3;

Scheme 1. Synthetic route of target compounds **7a**–**r**.

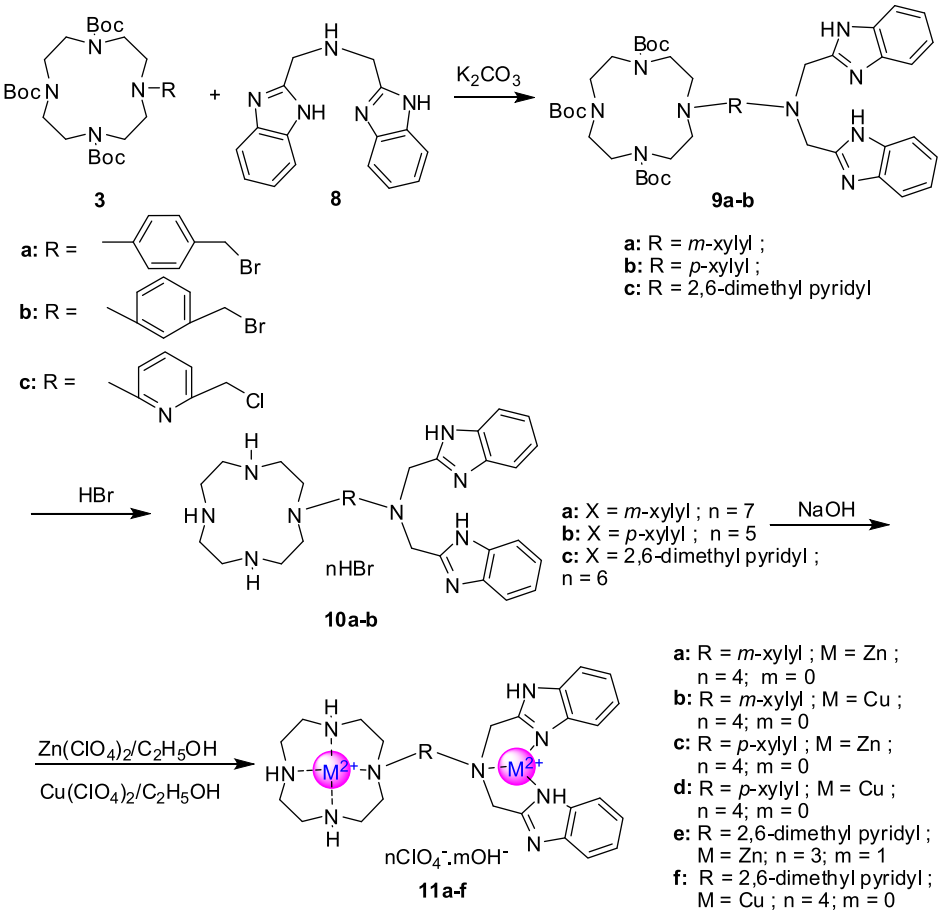

Scheme 2. Synthetic route of target compounds **11a**–**f**.

2. Results and discussion

2.1. Chemistry

The preparation of target derivatives were synthesized from 3Boc-cyclen. The reactions of protected cyclen with different halogenides, which were purified by column chromatography with ethyl acetate and petroleum ether (v/v = 1:2) as eluent. The azoles, such as **4a**–**d**, were reacted with **3a**–**b** on the conditions of NaH/THF or K_2CO_3/$CHCl_3$ to get the crude products **5a**–**l**, and the yields after being processed ranged from 22.6% to 95.3%. As for dinuclear ligands **9a**–**b** were efficiently prepared by substitution reaction between compound **3a**–**b** and IDB (N,N-bis(2-benzimidazolylmethyl)amine) (**8**) catalysed by K_2CO_3 in $CHCl_3$, then removed the residues by filtration and purified with column chromatography to get target materials, and the yields were 75.6%, 85.6% and 77.3% respectively. It must be pointed out that the solubility of IDB in $CHCl_3$ was poor, but the target material could dissolve in $CHCl_3$ very well. The reaction condition between IDB and compound **3** was mild and the basicity of K_2CO_3 was weaker than that of NaH, so that the reaction position in the IDB was the secondary amine. The residual two benzimidazole molecules could be used as ligand. Then compounds **5a**–**l** and **9a**–**b** were stirred with saturated HBr/C_2H_5OH, and their corresponding hydrobromates **6a**–**l** and **10a**–**b** were filtrated and collected. At last these compounds were dried in vacuo below 40 °C.

All these target complexes were produced followed the routes described below. The hydrobromide was dissolved in water (10 mL), and the pH of the solution was adjusted to 12 with aqueous NaOH. The alkaline solution was extracted with CH_2Cl_2 (30 mL × 5), then the solvent was dried by anhydrous Na_2SO_4 and evaporated. Solution of EtOH (10 mL), the obtained acid free ligand and equal/double molar weight of perchlorate were mixed and stirred at room temperature for 24 h. After that, the solid was filtered off, washed with cold EtOH, the residue was crystallized from H_2O/EtOH to obtained crystals, and the product was dried in vacuo. The synthetic route of target compounds were outlined in Schemes 1 and 2. The results of XRD tests shown in Fig. S1 in Supplementary information released that mono-nuclear complex **7c** and di-nuclear complex **11c** which was compared with its ligand **13** (shown in Scheme 3) could form crystal powder but no monocrystal was obtained.

It must be pointed out that the log K values of Cyclen and its pyridyl derivatives with Cu^{2+} were 23.4 and 24.0 respectively at the condition of $I = 1$ M in KNO_3, and stability constant (log K) of Cyclen with Zn^{2+} was 16.2 [19]. Meanwhile, the log *K* values of the other ligand IDB bonding with Cu^{2+} and Zn^{2+} were almost 6.34 and 5.96 at the condition of $I = 0.1$ M in KNO_3 [20], so its coordinative effect with Cu^{2+} or Zn^{2+} was also strong enough to interact with biomacromolecules in Tris–HCl buffer (pH 7.4) efficiently [21]. Further more, MS of compounds **7c** and **11a**–**f** dissolved in DMSO which was used as the solvent in the antibacterial assays were tested (shown in Fig. S2–Fig. S8 in Supplementary information) and each molecular ion peak could be found in the spectrogram, so it was also confirmed the stability of the target material.

2.2. Pharmacology

The *in vitro* antimicrobial screening for all synthesized compounds were evaluated for three Gram-positive bacteria (*Staphylococcus aureus* ATCC 6538, *Micrococcus luteus* ATCC 4698 and

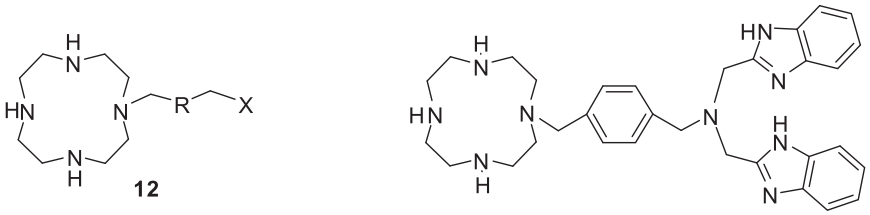

Scheme 3. The structures of selected ligands **12a**–**b** and **13**.

Bacillus subtilis ATCC 21216), three Gram-negative bacteria (*Escherichia coli* ATCC 8099, *Pseudomonas aeruginosa* ATCC 27853 and *Bacillus proteus* ATCC 13315) and two fungi (*Candida albicans* ATCC 76615 and *Aspergillus fumigatus* ATCC 96918) using two folds serial dilution technique recommended by National Committee for Clinical Laboratory Standards (NCCLS) with the positive control of clinically antimicrobial drugs Fluconazole and Chloromycin [22]. Minimal inhibitory concentration (MIC, μg/mL) was defined as the lowest concentration of new compounds that completely inhibited the growth of pathogenic microorganisms. The values of Clog *P* (a partition coefficient) were calculated using ChemDraw Ultra 10.0 software integrated with Cambridge Software (Cambridge Soft Corporation), and were depicted in Tables 1 and 2 respectively.

2.2.1. Antibacterial activity

The antibacterial results as shown in Table 1 revealed that most of the prepared mononuclear azole derivatives **7a**–**r** showed weak activities against Gram-positive bacteria *in vitro*, whereas some mononuclear compounds showed moderate efficacy against Gram-negative bacteria, especially for *B. proteus* or *P. aeruginosa*. Compound, such as **7g**, gave quite low inhibitory concentration (MIC = 8 μg/mL), which showed better inhibitory potency against *P. aeruginosa* than Chloromycin (MIC = 32 μg/mL) (Table 1). However its inhibitory potency against *B. proteus* (MIC = 32 μg/mL) was relatively weaker than the corresponding potency of Chloromycin (MIC = 2 μg/mL). Besides the imidazolyl complex **7g**, the MIC values of benzimidazolyl compounds **7e** and pyrazolyl compound **7h** against *B. proteus* were between 16 and 32 μg mL^{-1}. These results indicated that imidazolyl moiety seemed to be more helpful for the antibacterial activities than benzimidazolyl or other azole groups. Unfortunately, compounds like **7a** and **7b** containing imidazolyl groups showed no obvious inhibition antibacterial results and these MIC values were not shown in Table 1. Imidazolyl complexes having *m*-xylyl linkers showed better antibacterial activities, because the introduction of aryl chain with different length had remarkable effection on antibacterial activities, and it was unfavourable to place the imidazole too near or too far from the nucleus. As for imidazolyl complex **7m** with 2,6-dimethyl pyridyl linker, the nitrogen atom of pyridinyl ring in the complex might reduce the positive charge of Cu^{2+} [23], and could reduce the interaction between the cell membrane with negative charge and Cu^{2+} nucleus. Among these mononuclear salts, different cations in compounds didn't showed obviously different inhibitory potency.

To our surprise, the antibacterial results showed that compounds **11a**–**d** exhibited excellent efficacies against most of tested bacterial strains (Table 2). Particularly, compounds **11a**, **11b** with *m*-xylyl linker like **7g** displayed the best antibacterial activities, especially for *B. proteus* and *P. aeruginosa* with the MIC values ranging from 0.5 to 1 μg mL^{-1}, which was more potent than Chloromycin against the two strains with MIC values of 2 μg mL^{-1} and 32 μg mL^{-1} respectively. Results in Table 2 also demonstrated the significant influences of all sorts of aromatic linkers on biological activities. When the aromatic linkers changed to *p*-xylyl group, derivatives still exhibited moderate efficacies against tested bacteria, which were inferior to **11a** and **11b**. Complex **11d** showed inhibition potencies against Gram-positive bacteria *S. aureus* (MIC = 2 μg mL^{-1}), *M. luteu* (MIC = 2 μg mL^{-1}) and Gram-negative bacteria *P. aeruginosa* (MIC = 2 μg mL^{-1}), meanwhile the MIC values against these bacteria of Chloromycin was ranging from 2 μg mL^{-1} to 32 μg mL^{-1}. Regretfully, pyridyl-containing compounds **11e** and **11f** were unfavourable for the antibacterial efficiencies even at high concentration, this might be explained by the nitrogen atom of pyridine ring in complex reducing the positive charge density of each nucleus in **11e** and **11f**, which made both of them unfavourable for binding target sites. Therefore, suitable linker between two nuclei is necessary for the excellent antibacterial activities in drug design. As a comparison, antibacterial activities of some representative ligands **6f**, **12a**, **12b** and **13** (the structures of compounds **12a**, **12b** and **13** shown in Scheme 3) were tested, and they all showed weak antibacterial activities (shown in Table 3). It must be pointed out that complex **7g** which was composed of ligand **12a** and Cu^{2+}, and the MIC values of **7g** against *P. aeruginosa* and *B. proteus*. were 8 μg/mL and 32 μg/mL respectively which were much lower than that of **12a** ranging from 256 μg/mL to 512 μg/mL against this two kinds Gram-negative bacteria. Further more, the enhance effect was more significantly for complex with two metal ionic nuclei. So it could be concluded that the metal ion was the key factor for the antibacterial activity.

It could be concluded that the enhanced activities of dinuclear compound might be attributed to the better adhesion with electronegative member outside of bacteria for two cation nuclei, and the corresponding precursors **7e** and **7d** with only benzimidazole-pended and single cation nucleus showed no antibacterial activity. In a word, compounds **11a**–**c** displayed remarkable antibacterial activities, which indicated that they could be employed as potent novel board-spectrum antimicrobial agents for further study.

2.2.2. Antifungal activity

The *in vitro* antifungal evaluation of mononuclear complexes shown in Table 1 revealed that the activities of most compounds were relatively weak. However, the antifungal potencies of mononuclear compounds were more effective than their corresponding antibacterial properties. As for the compound **7l**, the inhibitory potency of *C. albicans* (MIC = 2 μg/mL) was comparable with the Fluconazole (MIC = 0.5 μg/mL) (Table 1). Meanwhile, complex **7c** also showed fine inhibitory potency against *C. albicans*, and its MIC value was 16 μg/mL. Especially to *A. fumigatus*, some mononuclear complexes showed comparable or even better inhibitory potencies than Fluconazole (MIC = 256 μg/mL), such as **7h** (MIC = 128 μg/mL) and **7j** (MIC = 64 μg/mL) (Table 1). The antifungal potencies of dinuclear compounds **11a**–**f** were far more better than their homologue mononuclear compounds. Compound such as **11a** gave

Table 1
The data of antimicrobial activities of mononuclear cyclen azole complexes and Clog *P* values.

Compds	Clog *P*	MIC_{50} (μg mL^{-1})							
		C. albicans	*A. fumigatus*	*M. luteus*	*S. aureus*	*B. subtilis*	*P. aeruginosa*	*B. proteus*	*E. coli*
7c	2.7389	16	>512	>512	>512	>512	512	>512	>512
7d	4.0630	256	512	>512	>512	>512	>512	64	>512
7e	3.8629	>512	128	128	>512	>512	>512	32	>512
7f	2.4689	512	256	>512	>512	>512	512	512	>512
7g	2.2689	256	256	>512	>512	512	8	32	512
7h	2.7389	64	128	>512	512	>512	128	16	>512
7i	2.5389	256	>512	>512	>512	>512	512	>512	>512
7j	4.0630	128	512	>512	>512	>512	512	>512	>512
7k	1.7391	64	64	>512	256	>512	>512	>512	>512
7l	1.5391	2	>512	512	>512	>512	>512	128	>512
7m	0.9720	512	512	>512	512	>512	256	512	>512
7n	1.2420	512	256	>512	>512	>512	256	512	>512
7o	0.2421	64	512	>512	>512	512	128	64	512
7q	2.5659	>512	512	256	>512	512	512	256	512
A	−1.09	–	–	2	8	4	32	2	4
B	−0.44	0.5	256		–	–		–	–

A: Chloromycin; B: Fluconazole.

quite low inhibitory concentration (MIC = 8 μg/mL) against *A. fumigatus*, which was 32-fold more effective than the first-line antifungal drug Fluconazole (MIC = 256 μg/mL), and the inhibitory potency of *C. albicans* (MIC = 0.5 μg/mL) was same as the Fluconazole (MIC = 0.5 μg/mL) (Table 2). To our surprise, all most newly synthesized dinuclear compounds, except **11e** and **11f**, displayed better or comparable antifungal activity with standard drug, and their MIC values were between 0.5 μg/mL and 128 μg/mL to against *C. albicans* and ranging from 8 μg/mL to 256 μg/mL for *A. fumigatus*. Target materials **11e** and **11f** were unfavourable for the antifungal efficiency, for that the nitrogen atom in pyridine might decrease the positive charge density on nucleus, and also impeded the approach between nucleus and fungus by electrostatic interactions. Like their antibacterial activities, the data in Tables 1 and 2 revealed that the inhibitory potencies of dinuclear compounds against fungi were much stronger than mononuclear analogue. At the same time, it could be found that complex coordinated Cu^{2+} showed better antifungal activity, and it could be explained by the oxygen radicals which enhanced the destructiveness originated from Cu^{2+}. To further explain the key effect of metal ion, we also test the antifungal activities of some representative ligands, such as compounds **6f**, **12a**, **12b** and **13**, and they showed weak antifungal activities (shown in Table 3). So that, it could be concluded that the metal ion was also the key factor for the antifungal activity.

Therefore, a significant structure–activity relationship could be concluded from these data to design the antifungal cyclen azole complex in future. Compounds with two nuclei conjugated azoles by *m*-xylyl groups and coordinated Cu^{2+} showed relative stronger antifungal potencies, and the length between two metal nuclei influenced the antimicrobial property greatly.

2.2.3. Effect of Clog P values on antimicrobial activity

These antimicrobial results could also be analysed by Clog *P* values. lipophilicity/hydrophilicity plays a significant role in determining where drugs are distributed and how rapidly they are metabolized and excreted in the body, for example, hydrophobic drugs are preferentially distributed to hydrophobic compartments such as lipid bilayers of cells while hydrophilic drugs are preferentially found in hydrophilic compartments like blood serum. For example, Fluconazole (Clog $P = -0.49$) with good water-solubility, had good hydrophilicity and could go into cytoplasm easily, and prohibited the P450 enzyme to synthesize ergosterol in fungus which induced fungus to death. Similarly, Chloromycin (Clog $P = -1.09$) also needed to enter into cytoplasm and binded 50S ribosomal subunit to interference the synthesis of protein in bacterial, and finally resulted bacterial to death. However, As seen from Table 2, all dinuclear compounds showed relative large Clog *P* values ranging from 4.9190 to 6.8159, it meaned that they could blend with lipid membrane conveniently and destruct the member of fungus straightly. And there was another key point needed to be mentioned, the two cationic nuclei could regulate the water-solubility appropriately at the same time, even the relative high positive charge density would also enhance the antifungal effect by reinforcing electrostatic interaction between the surface of microorganism and complex. So the proposed mechanism of antimicrobial activity of compounds **11a–d** might be quite different from Fluconazole or Chloromycin, and it proned to destroy the cell member like the quaternary ammonium salt antimicrobial agents [24]. Unlike the dinuclear compounds, Clog *P* values of the mononuclear compounds were ranging from 0.0421 to 4.0630 (Table 1), none of them were similar to either lipophilicity of the dinuclear compound or hydrophilicity of the standard drug, so that their antimicrobial activities were relatively poor. The Clog *P* values of cyclen azole complexes represented their antimicrobial efficiencies and were in accordance with the antimicrobial results discussed above.

2.3. Binding discussion

2.3.1. Fluorescence quenching mechanism

In this experiment, the concentration of BSA solution was 1.0×10^{-5} M, and the concentrations of compound **11b** solution increased progressively from 0 to 5.5×10^{-5} M at an increment of 0.5×10^{-5} M. The effect of compound **11b** on fluorescence of BSA intensity at 298 K was shown in Fig. 1A. It was observed that a gradual decrease of the fluorescence intensity was caused by the increment of compound **11b**, accompanied with the red shift of wavelength (from 345 to 352 nm) in the albumin spectrum. In Fig. 1A, the blue line showed the only emission spectrum of compound **11b**, which indicated that compound **11b** did not posses significant fluorescence feature, thus at the excitation wavelength (295 nm), the effect of compound **11b** on fluorescence of BSA could be negligible. The decreased fluorescence intensity is usually described by the Stern–Volmer [25] equation:

Table 2
The data of antimicrobial activities of dinuclear cyclen complexes and Clog *P* values.

Compds	Clog *P*	MIC_{50} (μg mL^{-1})							
		C. albicans	*A. fumigatus*	*M. luteus*	*S. aureus*	*B. subtilis*	*P. aeruginosa*	*B. proteus*	*E. coli*
11a	6.8159	0.5	8	8	16	32	1	0.5	256
11b	6.4160	1	16	16	64	128	>512	1	64
11c	6.8159	128	8	8	256	128	>512	4	64
11d	6.4160	16	8	2	2	64	2	>512	32
11e	5.3190	64	256	>512	512	256	128	64	512
11f	4.9190	256	>512	>512	>512	512	512	256	>512
A	−1.09	–	–	2	8	4	32	2	4
B	−0.44	0.5	256		–	–	–	–	–

A: Chloromycin; B: Fluconazole.

Table 3
The data of antimicrobial activities of ligands and their Clog *P* values.

Compds	Clog *P*	MIC_{50} (μg mL^{-1})							
		C. albicans	*A. fumigatus*	*M. luteus*	*S. aureus*	*B. subtilis*	*P. aeruginosa*	*B. proteus*	*E. coli*
6f	−0.726	256	512	256	>512	>512	>512	>512	256
12a	0.004	256	256	256	512	512	256	512	126
12b	0.101	128	256	512	>512	>512	512	512	512
13	1.22	64	128	512	128	512	256	256	512
A	−1.09	–	–	8	8	8	4	8	2
B	−0.44	4	256		–	–	–	–	–

A: Chloromycin; B: Fluconazole.

$$\frac{F_0}{F} = 1 + K_{SV}[Q] \quad (1)$$

In this equation the F_0 and F represent steady-state fluorescence intensities in the absence and presence of compound **11b**, respectively. K_{SV} is the Stern–Volmer quenching constant, and [Q] is the concentration of compound **11b**. Hence, K_{SV} was calculated by linear regression of plot of F_0/F versus [Q] (Fig. 1B–D). Quenching mechanisms are often classified as dynamic quenching, static quenching etc. depending on temperature and viscosity. Because higher temperatures result in larger diffusion coefficients, the quenching constants are expected to increase with a gradually increasing temperature in dynamic quenching. However, the increasing of temperature is likely to result in a smaller static quenching constant due to the dissociation of weakly bound complexes [26]. Therefore, the K_{SV} was calculated from Stern–Volmer plots at each temperature. The results (Table 4) demonstrated that the quenching constant K_{SV} was inversely correlated with temperature, which indicated that the probable quenching mechanism of compound **11b**-BSA binding reaction was initiated by ground-state complex formation (static quenching) [27].

2.3.2. Binding constant

For a static quenching procedure, the data was analysed according to the Modified Stern–Volmer [28] equation:

$$\frac{F_0}{\Delta F} = \frac{1}{f_a K_a}\frac{1}{[Q]} + \frac{1}{f_a} \quad (2)$$

ΔF is the difference of fluorescence in the absence and presence of compound **11b** at concentration [Q], f_a is the fraction of accessible fluorescence, and K_a is the effective quenching constant for the accessible fluorophores. The dependence of $F_0/\Delta F$ on the reciprocal value of concentration $[Q]^{-1}$ is linear with the slope equalling to the value of $(f_a K_a)^{-1}$. The Modified Stern–Volmer plots were Fig. 2 and the calculated results were depicted in Table 5. Fig. 2 showed the Modified Stern–Volmer and Scatchard plots for the compound **11b**-BSA system at different temperatures. The decreasing trend of K_a with increasing temperatures was in accordance with K_{SV}'s dependence on temperatures. Moreover, the interaction between BSA and compound **11b** accelerated with the temperature increasing, hence the high affinity binding sites of the interaction were slightly strengthened, which were accordance with the results shown in Table 5. The results also showed that the binding constant was moderate and the effect of temperature was not significant, thus compound **11b** might be stored and carried by this protein [28].

2.3.3. Binding mode and thermodynamic parameters

The interaction forces between bioactive small molecules or drugs and biomolecules include electrostatic interactions, multiple hydrogen bonds, van der Waals interactions, hydrophobic and steric contacts within the antibody-binding site and so on. If the enthalpy change (ΔH) does not vary significantly over the studied temperature range, then its value and that of entropy change (ΔS) can be evaluated from the van't Hoff equation:

$$LnK = -\frac{\Delta H}{RT} + \frac{\Delta S}{R} \quad (3)$$

K is analogous to the associative binding constants at the corresponding temperature and R is the gas constant. In order to explain the interaction between compound **11b** and BSA, the thermodynamic parameters were calculated from the van't Hoff plots. The enthalpy change (ΔH) was estimated from the slope of the van't Hoff relationship (Fig. 3). The free energy change (ΔG) was then calculated from the following equation:

$$\Delta G = \Delta H - T\Delta S \quad (4)$$

Table 6 summarized the values of ΔH, ΔG and ΔS. The negative values of free energy ΔG suggested the binding process was

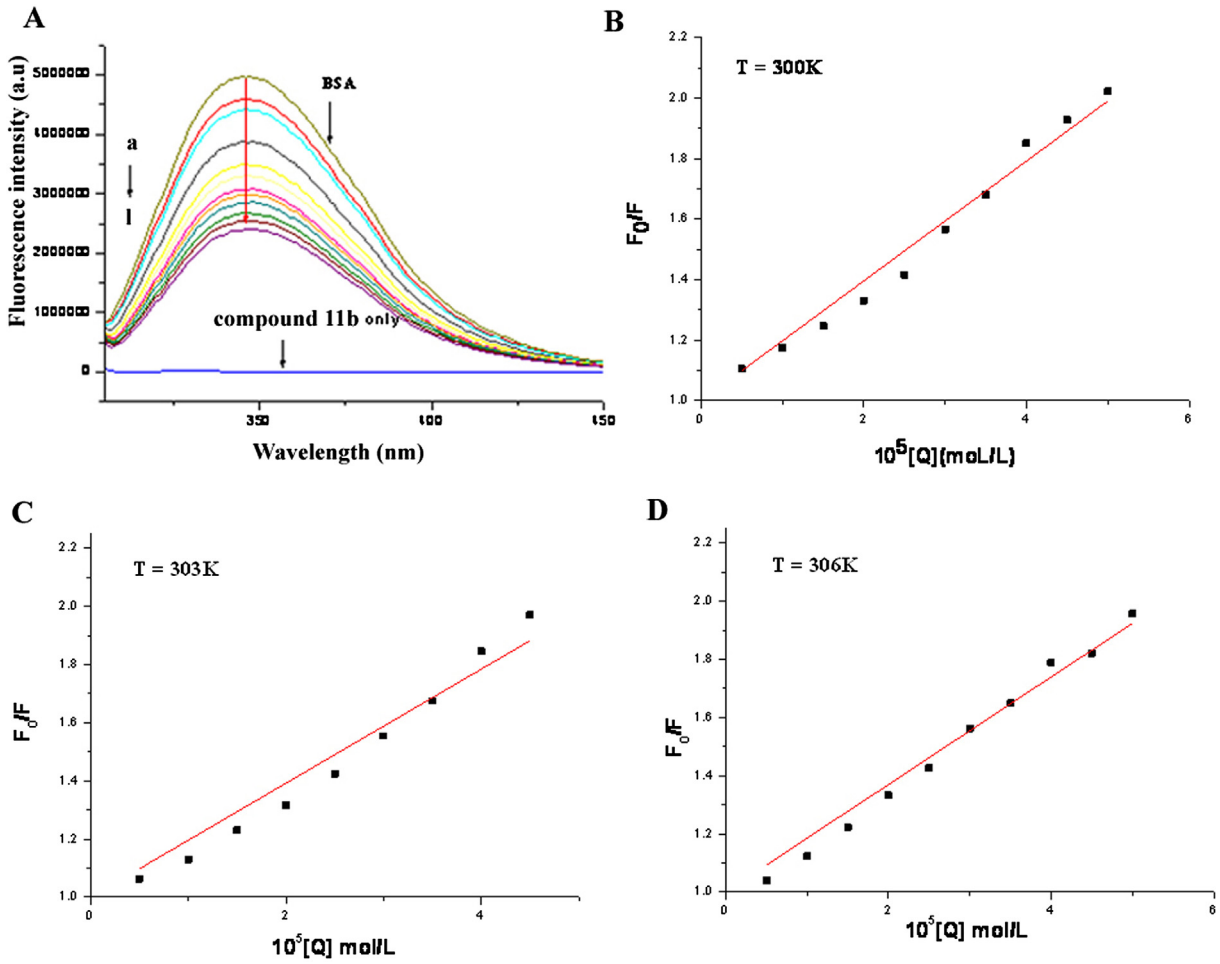

Fig. 1. (A) Emission spectra of BSA in the presence of various concentrations of compound **11b**. c(BSA) 1.0×10^{-5} M; c(compound **11b**)/(10^{-5} M), **a**–**l**: from 0.0 to 5.5 at increments of 0.50; blue line shows the emission spectrum of compound **11b** only; $T = 298$ K, $\lambda_{ex} = 295$ nm. (B–D) Stern–Volmer plot of **11b**-BSA at three different temperatures. (For interpretation of the references to colour in this figure legend, the reader is referred to the web version of this article.)

spontaneous, the negative entropy ΔS and enthalpy ΔH values of the interaction of compound **11b** with BSA indicated that the binding was mainly enthalpy-driven and the entropy was unfavourable for it, moreover, hydrogen bonds and van der Waals forces played a major role in the reaction [29].

2.4. Cytotoxicity

The cytotoxic activities of these complexes were tested by CCK8 method. The *in vitro* cytotoxicity was evaluated in HL-7702 cells. As shown in Fig. 4, none of them displayed serious cytotoxicity in this cell-line and the relative cell viability of **11a**, **11c**, **11e** were more than 70% when its concentration was over 100 μg/mL. To our surprise, three Cu^{2+} complexes showed relative high cytotoxicity in the cell-line. Data obtained from *in vitro* and cell culture studies were largely supportive of copper's capacity to initiate oxidative damage and interfere with important cellular events [30]. But the results also reflected that all of these complexes **11a**–**f** showed relative low toxicity to normal human hepatic cells at high concentration. And especially at the dose of MIC to several kinds of pathogenic microorganisms, dinuclear compounds were still safe for use.

3. Conclusion

In conclusion, all the new compounds were characterized by ^{1}H NMR, MS, and elemental analysis spectra. The *in vitro* antimicrobial activities of these azole cyclen derivatives were evaluated against six bacterial strains and two fungal strains. The biological results revealed that the most mono-nucleus complexes exhibited poor or no biological activities, some compounds such as **7g** (MIC = 8 μg/mL against *P. aeruginosa*) and **7l** (MIC = 2 μg/mL against *C. albicans*) showed moderate antibacterial and antifungal activities respectively. Meanwhile, most of newly synthesized di-nuclei compounds **11** displayed moderate to excellent antibacterial and antifungal activities against all the tested strains compared to the reference drugs Chloromycin and Fluconazole. Compounds **11a**–**d** with aromatic chains gave better antimicrobial efficiency than compounds **11e**–**f** incorporated pyridyl groups, especially for *m*-xylyl linked compounds **11a** and **11b** which exhibited the best bacterial growth inhibitory activities. The MIC value of **11a** against *P. aeruginosa* was 1 μg/mL, and the MIC values of **11a** and **11b** against *B. proteus* were 0.5 μg/mL and 1 μg/mL respectively, which were 4–12 fold to that of Chloromycin. As for antifungal activity, the MIC values of **11a** and **11b** against *A. fumigatus* were 8 μg/mL and 16 μg/mL, and it indicated 16–32 fold to the MIC values of Fluconazole. And it also could be concluded that the metal ion was the key factor for the antimicrobial activity, especially for the complexes with two nuclei.

The specific interaction of compound **11b** with BSA was studied by fluorescence spectroscopy. The experimental results displayed that the quenching mechanism of fluorescence of BSA by compound **11b** was a static quenching procedure, binding constant and binding sites were obtained according to the classical equations.

Table 4
Stern–Volmer quenching constants for the interaction of compound **11b** with BSA at various temperatures.

pH	T (K)	10^{-4} K_{sv}/(L/moL)	R[a]	Standard error
7.4	300	0.198	0.989	0.00485
7.4	303	0.196	0.979	0.00762
7.4	306	0.185	0.991	0.0043

[a] Is the correlation coefficient.

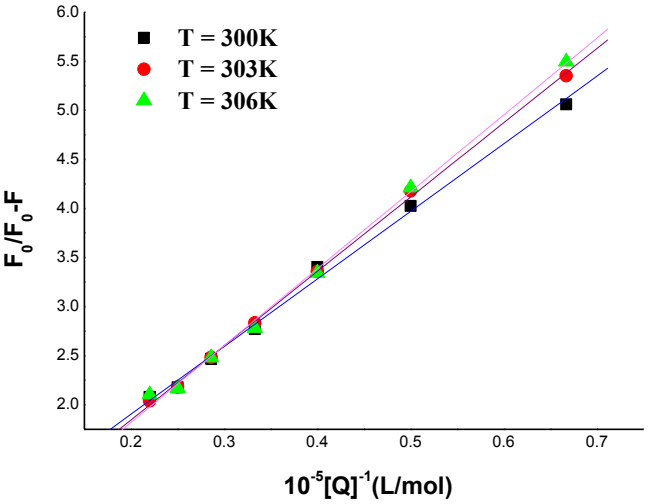

Fig. 2. Modified Stern–Volmer plots of compound **11b**-BSA system at different temperatures.

Table 5
Modified Stern–Volmer quenching constants for the interaction of compound **11b** with BSA at various temperatures.

pH	T (K)	10^{-4} K_a/(L/moL)	R[a]	S.D.[b]
7.4	300	0.765	0.998	0.07879
7.4	303	0.431	0.999	0.03979
7.4	306	0.324	0.998	0.07545

[a] Is the correlation coefficient.
[b] Is standard deviation.

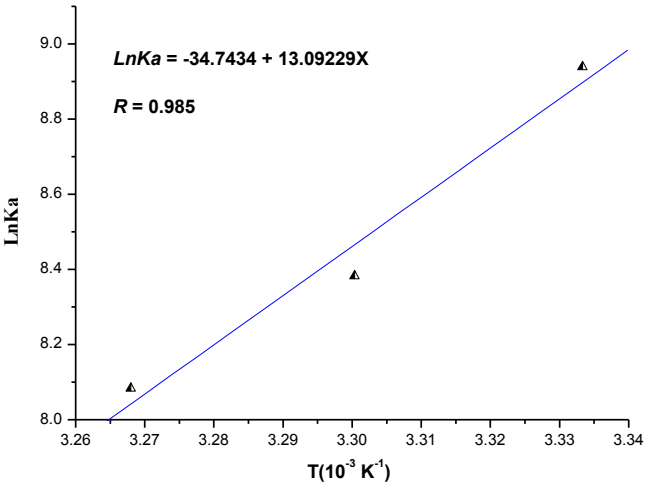

Fig. 3. Van't Hoff plots of compound **11b**-BSA system.

The thermodynamic parameters indicated that the binding process was spontaneous, the negative entropy ΔS and enthalpy ΔH values of the interaction of compound **11b** and BSA suggested that the binding should be mainly enthalpy-driven and the entropy was unfavourable for it, moreover, hydrogen bonds and van der Waals forces played major roles in the interaction. The CCK-8 tests certified that the cytotoxicities of these effective compounds **11a**–**d** were low. These results indicate that the new type of antimicrobial complexes could be a series of promising reagents for further exploitation.

4. Experimental protocols

4.1. General methods

Melting points were uncorrected and recorded on X-6 melting point apparatus without any corrections. TLC analysis was done using pre-coated silica gel plates. All of reagents and solvents used were commercially available without further purification. MS spectra data were recorded on Finnigan MAT-4510 and VG Auto 3000 mass spectrometer and Agilent 6200 LCMS-IT-TOF mass spectrometer, respectively. ^{1}H NMR spectra were recorded on Brucker AV-300 and AV-400. MHz and chemical shifts are reported relative to internal Me_4Si. Elemental analyses were performed by using a Carlo-Elba 1106 elemental analytical instrument. XRD data were tested by Shimazduo DIFFRACTOMETER-6000. $CHCl_3$ and THF were purified according to the standard method. N, N-Diisopropylethylamine (DIPEA) and Halides **2a**–**c** were purchased from Sigma or prepared follow the reference (Supplementary information). All aqueous solutions were prepared using deionized and redistilled water. All other chemicals and solvents were commercially available, and were used without further purification.

All fluorescence spectra were recorded on Horiba Jobin Yvon Fluoromax-4 spectrofluorometer; corrected for the system response equipped with 1.0 cm quartz cells, the widths of both the excitation and emission slit were set as 2.5 nm, and the excitation wavelength was 295 nm. Fluorescence spectra were recorded at 298, 300, 303, 306 K in the range of 300–450 nm. The temperature were controlled with PolyScience temperature controller. The BSA was obtained from Sigma–Aldrich (St. Louis, MO, USA). Tris, NaCl, HCl, ethanol were analytical purity. BSA was dissolved in Tris–HCl buffer solution (0.05 M Tris, 0.15 M NaCl, pH = 7.4), compound **11b** was dissolved in redistilled water [31].

4.1.1. Synthesis of compounds *1*–*6*, *9*–*10*, *12* and *13*

Compounds **1**–**6**, **9**–**10**, **12** and **13** were prepared according to the literature procedures [32] (Supplementary information).

4.1.2. Synthesis of compounds *7* and *11*

General procedure of the syntheses of **7** and **11**. The obtained acid free ligand and equal or double molar weight of $Zn(ClO_4)_2{\cdot}6H_2O$ or $Cu(ClO_4)_2{\cdot}6H_2O$ were stirred at room temperature for 24 h. After that, the solids were filtered off, washed with cooled EtOH, the residue was crystallized from H_2O/EtOH to obtained colourless crystals. The product was dried in vacuo. Data of compounds **7a**–**r** were shown in Supplementary information.

Table 6
Thermodynamic parameters of compound **11b**-BSA interaction at different temperatures.

T (K)	△H (kJ/mol)	△G (kJ/mol)	△S (J/moL K)
300	−108.78	−22.16	−288.72
303		−21.30	
306		−20.43	

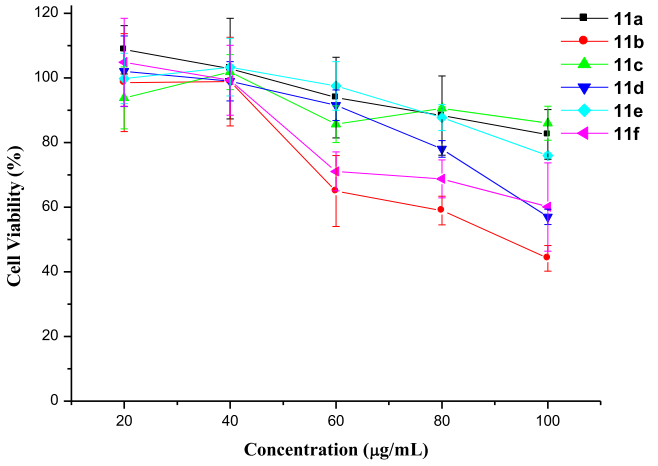

Fig. 4. Relative cell viabilities of compounds **11a**–**f** in HL-7702 cells.

*4.1.2.1. N-(3-((1,4,7,10-Tetraazacyclododecan-1-yl)methyl)benzyl)-N-((1H-benzo[d]imidazol-2-yl)methyl)-1-(1H-benzo[d]imidazol-2-yl) methanamine Zn(II) complex (**11a**).* A solution of EtOH (10 mL), the obtained acid free ligand (0.17 g, 0.32 mmoL) and $Zn(ClO_4)_2\cdot 6H_2O$ (0.24 g, 0.65 mmo1) was stirred at room temperature for 24 h. After that, the process followed the procedure described above. White solid (yield 29.3%). m.p. 265–267 °C. MS(ESI) *m/z*: 714.2311 [$(M+K^+ - 4H^+ - 4ClO_4^-)$], 752.1704 [$(M+2K^+ - 5H^+ - 4ClO_4^-)$]. Anal. Calcd. for $C_{32}H_{41}Cl_4N_9O_{16}Zn_2\cdot 5H_2O$: C 32.84, H 4.39, N 10.77; found: C 32.78, H 4.45, N 10.10. ^{1}H NMR (d_6-DMSO, 300 MHz) δ: 2.51–3.06 (br, 16H, NC*H*$_2$C*H*$_2$N), 3.44–3.49 (br, 2H, CyclenC*H*$_2$Py), 4.07 (s, 2H, NC*H*$_2$Py), 4.31 (br, 4H, C*H*$_2$BIm), 7.13 (br, 2H, BIm-*H*), 7.30–7.87 (m, 12H, Py-*H*, BIm-*H*).

*4.1.2.2. N-(3-((1,4,7,10-Tetraazacyclododecan-1-yl)methyl)benzyl)-N-((1H-benzo[d]imidazol-2-yl)methyl)-1-(1H-benzo[d]imidazol-2-yl)methanamine Cu(II) complex (**11b**).* A solution of EtOH (10 mL), the obtained acid free ligand (0.17 g, 0.32 mmoL) and $Cu(ClO_4)_2\cdot 6H_2O$ (0.24 g, 0.65 mmo1) was stirred at room temperature for 24 h. After that, the process followed the procedure described above. Blue solid (yield 58.7%). m.p. 254–256 °C. MS(ESI) *m/z*: 697 [$(M+Na^+ - 4H^+ - 4ClO_4^-)$, 61]. Anal. Calcd. for $C_{32}H_{41}Cl_4N_9O_{16}Cu_2\cdot C_2H_5OH$: C 36.37, H 4.22, N 11.32; found: 36.48, H 4.49, N 10.99.

*4.1.2.3. N-(4-((1,4,7,10-Tetraazacyclododecan-1-yl)methyl)benzyl)-N-((1H-benzo[d]imidazol-2-yl)methyl)-1-(1H-benzo[d]imidazol-2-yl)methanamine Zn(II) complex (**11c**).* A solution of EtOH (10 mL), the obtained acid free ligand (0.16 g, 0.29 mmoL) and $Zn(ClO_4)_2\cdot 6H_2O$ (0.22 g, 0.60 mmo1) was stirred at room temperature for 24 h. After that, the process followed the procedure described above. White solid (yield 45.6%). m.p. 255–257 °C. MS(ESI) *m/z*: 752.1786 [$(M+2K^+ - 5H^+ - 4ClO_4^-)^+$], 818.1784 [$(M+K^+ - 3H^+ - 3ClO_4^-)^+$]. Anal. Calcd. for $C_{32}H_{41}Cl_4N_9O_{16}Zn_2\cdot 3H_2O$: C 33.88, H 4.18, N 11.11; found: C 34.11, H 4.47, N 10.77. ^{1}H NMR (d_6-DMSO, 300 MHz) δ: 2.69–3.10 (br, 16H, NC*H*$_2$C*H*$_2$N), 3.62 (s, 2H, CyclenC*H*$_2$Py), 4.08 (s, 2H, NC*H*$_2$Py), 4.33 (br, 4H, C*H*$_2$BIm), 6.95–6.97 (br, 2H, BIm-*H*), 7.30–7.77 (m, 12H, Py-*H*, BIm-*H*). ^{13}C NMR (d_6-DMSO, 100 MHz) δ: 42.20, 43.77, 44.68, 53.39, 60.84, 63.33, 100.92, 103.40, 114.53, 118.01, 122.66, 123.85, 124.17, 131.61, 135.05.

*4.1.2.4. N-(4-((1,4,7,10-Tetraazacyclododecan-1-yl)methyl)benzyl)-N-((1H-benzo[d]imidazol-2-yl)methyl)-1-(1H-benzo[d]imidazol-2-yl)methanamine Cu(II) complex (**11d**).* A solution of EtOH (10 mL), the obtained acid free ligand (0.16 g, 0.29 mmoL) and $Cu(ClO_4)_2\cdot 6H_2O$ (0.22 g, 0.60 mmoL) was stirred at room temperature for 24 h. After that, the process followed the procedure described above. Blue solid (yield 37.3%). m.p. 267–271 °C. MS(ESI) *m/z*: 674 [$(M - 3H^+ - 4ClO_4^-)^+$, 100]. Anal. Calcd. for $C_{32}H_{41}Cl_4N_9O_{16}Cu_2\cdot 2H_2O$: C 34.54, H 4.08, N 11.42; found: C 34.96, H 4.05, N 11.02.

*4.1.2.5. 1-(6-((1,4,7,10-Tetraazacyclododecan-1-yl)methyl)pyridin-2-yl)-N,N-bis((1H-benzo[d]imidazol-2-yl)methyl)methanamine Zn(II) complex (**11e**).* A solution of EtOH (10 mL), the obtained acid free ligand (0.17 g, 0.32 mmoL) and $Zn(ClO_4)_2\cdot 6H_2O$ (0.24 g, 0.65 mmoL) was stirred at room temperature for 24 h. After that, the process followed the procedure described above. White solid (yield 31.3%). m.p. 273–275 °C. MS(ESI) *m/z*: 715.2184 [$(M+K^+ - 4H^+ - OH^- - 3ClO_4^-)^+$], 817.1693 [$(M+K^+ - 3H^+ - OH^- - 2ClO_4^-)^+$]. Anal. Calcd. for $C_{31}H_{42}Cl_3N_{10}O_{13}Zn_2\cdot H_2O$: C 36.58, H 4.36, N 13.76; found: C 36.87, H 4.64, N 13.33. ^{13}C NMR (d_6-DMSO, 100 MHz) δ: 46.55, 53.70, 76.03, 85.36, 112.66, 115.12, 119.18, 122.27, 137.54, 153.34.

*4.1.2.6. 1-(6-((1,4,7,10-Tetraazacyclododecan-1-yl)methyl)pyridin-2-yl)-N,N-bis((1H-benzo[d]imidazol-2-yl)methyl)methanamine Cu(II) complex (**11f**).* A solution of EtOH (10 mL), the obtained acid free ligand (0.17 g, 0.32 mmoL) and $Cu(ClO_4)_2\cdot 6H_2O$ (0.24 g, 0.65 mmoL) was stirred at room temperature for 24 h. After that, the process followed the procedure described above. Blue solid (yield 58.5%). m.p. > 247 °C (dec). MS(ESI) *m/z*: 714.2190 [$(M+K^+ - 4H^+ - 4ClO_4^-)^+$], 816.1904 [$(M+K^+ - 3H^+ - 3ClO_4^-)^+$], Anal. Calcd. for $C_{31}H_{40}Cl_4N_{10}O_{16}Cu_2\cdot C_2H_5OH$: 35.27, H 4.13, N 12.47; found: C 35.72, H 4.49, N 12.58.

4.2. Antibacterial and antifungal assays

The *in vitro* minimal inhibitory concentrations (MICs) of the target compounds were determined using the two-fold serial dilution technique in 96-well microtest plates according to the National Committee for Clinical Laboratory Standards. The tested microorganism strains were provided by the School of Pharmaceutical Sciences, Southwest University and the College of Pharmacy, Third Military Medical University. Chloromycin and Fluconazole were used as standard drugs.

4.2.1. Antibacterial assays

The prepared compounds **7a**–**r** and **11a**–**f** were evaluated for their antibacterial activities against *S. aureus* ATCC 6538, *M. luteus* ATCC 4698 and *B. subtilis* ATCC 21216 as Gram-positive, *E. coli* ATCC 8099, *P. aeruginosa* ATCC 27853 and *B. proteus* ATCC 13315 as Gram-negative bacteria. The bacterial suspension was adjusted with sterile saline to a concentration of 1×10^{-5} CFU. The tested compounds were dissolved in DMSO to prepare the stock solutions. The tested compounds and reference drugs were prepared in Mueller-Hinton broth (Guangdong huaikai microbial sci.& tech co., Ltd, Guangzhou, Guangdong, China) by two-fold serial dilution to obtain the required concentrations of 512, 256, 128, 64, 32, 16, 8, 4, 2, 1, 0.5 μg/mL. These dilutions were inoculated and incubated at 37 °C for 24 h. To ensure that the solvent had no effect on bacterial growth, a control test was performed with test medium supplemented with DMSO at the same dilutions as used in the experiment.

4.2.2. Antifungal assays

The newly synthesized compounds were evaluated for their antifungal activity against *C. albicans* ATCC 76615 and *A. fumigatus* ATCC 96918. A spore suspension in sterile distilled water was

prepared from 1-day old culture of the fungi growing on Sabouraud agar (SA) media. The final spore concentration was $1–5 \times 10^3$ spore mL^{-1}. From the stock solutions of the tested compounds and reference antifungal Fluconazole, dilutions in sterile RPMI 1640 medium (Neuronbc Laboraton Technology CO., Ltd, Beijing, China) were made resulting in eleven desired concentrations (0.5–512 μg/mL) of each tested compound. These dilutions were inoculated and incubated at 37 °C for 24 h. The drug MIC was defined as the first well with an approximate 80% reduction in growth compared to the growth of the drug-free well. The minimum inhibitory concentration values (MICs) (in μg/mL) were summarized in Tables 1 and 2.

4.3. Cell viability assay

Toxicity of **11a**–**f** toward HL-7702 cells was determined by using Cell Counting Kit-8 (CCK8, Yeasen Company) based on WST-8 (4-(3-(2-methoxy-4-nitrophenyl)-2-(4-nitrophenyl)-2H-tetraz-ol-3-ium-5-yl)benzene-1,3-disulfonate) reduction assay following literature procedures [33]. The HL-7702 cells (6000 cells per well) were seeded into 96-well plates. The cells were then incubated in a culture medium containing **11a**–**f** with a particular concentration for 24 h. After that, 10 μL of CCK8 was added to each well. After 4 h, the unreacted dye was removed by aspiration. The OD value were measured spectrophotometrically in an ELISA plate reader (model 550, Bio-Rad) at a wavelength of 450 nm. The cell survival was expressed as follows: cell viability = (OD treated/OD control) × 100%. The results were shown in Fig. 4.

Acknowledgements

This work was financially supported by Natural Science Foundation Project of CQ CSTC (cstc2013jcyjA50012), Scientific and Technological Research Program of Chongqing Municipal Education Commission (Grant No. KJ130820), the New Teacher Foundation of Chongqing University of Technology (2012ZD24), and National Science Foundation of China (No. 21173274).

Appendix A. Supplementary data

Supplementary data related to this article can be found at http://dx.doi.org/10.1016/j.ejmech.2014.07.075.

References

[1] K.K. Kumarasamy, M.A. Toleman, T.R. Walsh, J. Bagaria, F. Butt, R. Balakrishnan, U. Chaudhary, M. Doumith, C.G. Giske, S. Irfan, P. Krishnan, A.V. Kumar, S. Maharjan, S. Mushtaq, T. Noorie, D.L. Paterson, A. Pearson, C. Perry, R. Pike, B. Rao, U. Ray, J.B. Sarma, M. Sharma, E. Sheridan, M.A. Thirunarayan, J. Turton, S. Upadhyay, M. Warner, W. Welfare, D.M. Livermore, N. Woodford, Lancet Infect. Dis. 10 (2010) 597–602.
[2] J. Valdez, R. Cedillo, A. Hernández-Campos, L. Yépez, F. Hernández-Luis, G. Navarrete-Vázquez, A. Tapia, R. Cortés, M. Hernández, R. Castillo, Bioorg. Med. Chem. Lett. 12 (2002) 2221–2224.
[3] R. Iemura, T. Kawashima, T. Fukuda, K. Ito, G. Tsukamoto, J. Med. Chem. 29 (1986) 1178–1183.
[4] Y.S. Tong, J.J. Bouska, P.A. Ellis, E.F. Johnson, J. Leverson, X.S. Liu, P.A. Marcotte, A.M. Olson, D.J. Osterling, M. Przytulinska, L.E. Rodriguez, Y. Shi, N. Soni, J. Stavropoulos, S. Thomas, C.K. Donawho, D.J. Frost, Y. Luo, V.L. Giranda, T.D. Penning, J. Med. Chem. 52 (2009) 6803–6813.
[5] Y.F. Li, G.F. Wang, P.L. He, W.G. Huang, F.H. Zhu, H.Y. Gao, W. Tang, Y. Luo, C.L. Feng, L.P. Shi, Y.D. Ren, W. Lu, J.P. Zuo, J. Med. Chem. 49 (2006) 4790–4794.
[6] K.C.S. Achar, K.M. Hosamani, H.R. Seetharamareddy, Eur. J. Med. Chem. 45 (2010) 2048–2054.
[7] C.L. Sann, A. Baron, J. Mann, H.V.D. Berg, M. Gunaratnam, S. Neidle, Org. Biomol. Chem. 4 (2006) 1305–1312.
[8] T. Kálai, M. Balog, A. Szabó, G. Gulyás, J. Jeko, B. Sümegi, K. Hideg, J. Med. Chem. 52 (2009) 1619–1629.
[9] W.W.K.R. Mederski, D. Dorsch, S. Anzali, J. Gleitz, B. Cezanne, C. Tsaklakidis, Bioorg. Med. Chem. Lett. 14 (2004) 3763–3769.
[10] C. Gill, G. Jadhav, M. Shaikh, R. Kale, A. Ghawalkar, D. Nagargoje, M. Shiradkar, Bioorg. Med. Chem. Lett. 18 (2008) 6244–6247.
[11] S.A.F. Rostom, H.M.A. Ashour, H.A.A.E. Razik, A.E.F.H.A.E. Fattah, N.N. El-Din, Bioorg. Med. Chem. 17 (2009) 2410–2422.
[12] [a] C.H. Zhou, Y. Wang, Curr. Med. Chem. 19 (2012) 239–280;
[b] Y. Wang, C.H. Zhou, Sci. Sin. Chim. 41 (2011) 1429–1456 (in Chinese).
[13] L. Zhang, Y. Ling, M. Du, Inorg. Chim. Acta 360 (2007) 3182–3188.
[14] N.M. Aghatabay, A. Neshat, T. Karabiyik, M. Somer, D. Haciu, B. Dülger, Eur. J. Med. Chem. 42 (2007) 205–213.
[15] [a] O. Andersen, Chem. Rev. 99 (1999) 2683–2710;
[b] C.J. Anderson, M.J. Welch, Chem. Rev. 99 (1999) 2219–2234;
[c] P. Caravan, J.J. Ellison, T.J. McMurry, R.B. Lauffer, Chem. Rev. 99 (1999) 2293–2352;
[d] D. Parker, Chem. Soc. Rev. 19 (1990) 271–291.
[16] [a] P. Failli, D. Bani, A. Bencini, M. Cantore, L.D.C. Mannelli, C. Ghelardini, C. Giorgi, M. Innocenti, F. Rugi, A. Spepi, R. Udisti, B. Valtancoli, J. Med. Chem. 52 (2009) 7273–7283;
[b] D.P. Singh, R. Kumar, J. Singh, Eur. J. Med. Chem. 44 (2009) 1731–1736;
[c] G. Nirmala, A.K. Rahiman, S. Sreedaran, R. Jegadeesh, N. Raaman, V. Narayanan, Spectrochim. Acta. Part. A 77 (2010) 92–100;
[d] S. David, D. Ordway, M.-J. Arroz, J. Costa, R. Delgado, Res. Microbiol. 152 (2001) 569–576;
[e] D.A. Knight, T.E. Hickey, J.E. Bongard, D.C. Thach, R. Yngard, E.L. Chang, J. Inorg. Biochem. 104 (2010) 592–598.
[17] J.B. Bremner, J.I. Ambrus, S. Samosorn, Curr. Med. Chem. 14 (2007) 1459–1477.
[18] [a] D. Agudelo, P. Bourassa, J. Bruneau, G. Berube, É. Asselin, H.A. Tajmir-Riahi, PLoS One 8 (2012) e43814;
[b] N. Kamtekar, A. Pandey, N. Agrawal, R.R.S. Pissurlenkar, M. Borana, B. Ahmad, PLoS One 8 (2013) e53499;
[c] A. Belatik, S. Hotchandani, J. Bariyanga, H.A. Tajmir-Riahi, Eur. J. Med. Chem. 48 (2012) 114–123.
[19] L.M.P. Lima, D. Esteban-Gómez, R. Delgado, C. Platas-Iglesias, R. Tripier, Inorg. Chem. 51 (2012) 6916–6927.
[20] R.W. Hay, T. Clifford, P. Lightfoot, Polyhedron l7 (1998) 3575–3581.
[21] X.G. Meng, L. Liu, C.S. Zhou, L. Wang, C.L. Liu, Inorg. Chem. 47 (2008) 6572–6574.
[22] National Committee for Clinical Laboratory Standards Approved standard Document, M27–A2, Reference Method for Broth Dilution Antifungal Susceptibility Testing of Yeasts, National Committee for Clinical LaboratoryStandards, Wayne, PA, 2002.
[23] Q.X. Xiang, X.Q. Yu, J. Wu, P.Y. Liu, C.Q. Xia, R.G. Xie, Chin. J. Chem. 21 (2003) 910–916.
[24] E.R. Kenawy, Y.A.-G. Mahmoud, Macromol. Biosci. 3 (2003) 107–116.
[25] J.R. Lakowicz, Principles of Fluorescence Spectroscopy, third ed., Springer, New York, 2006, pp. 11–12.
[26] N. Ibrahim, H. Ibrahim, S. Kim, J.P. Nallet, F. Nepveu, Biomacromolecules 11 (2010) 3341–3351.
[27] Y.-J. Hu, Y. Ou-Yang, C.-M. Dai, Y. Liu, X.-H. Xiao, Biomacromolecules 11 (2010) 106–112.
[28] S.S. Lehrer, Biochemistry 10 (1971) 3254–3263.
[29] D.P. Ross, S. Subramanian, Biochemistry 20 (1981) 3096–3102.
[30] L.M. Gaetke, C.K. Chow, Toxicology 189 (2003) 147–163.
[31] Y.Z. Zhang, B. Zhou, Y.X. Liu, C.X. Zhou, X.L. Ding, Y. Liu, J. Fluoresc. 18 (2008) 109–118.
[32] C.Q. Xia, N. Jiang, J. Zhang, S.Y. Chen, H.H. Lin, X.Y. Tan, Y. Yue, X.Q. Yu, Bioorg. Med. Chem. 14 (2006) 5756–5764.
[33] J.E. Frith, D.J. Menzies, A.R. Cameron, P. Ghosh, D.L. Whitehead, S. Gronthos, A.C.W. Zannettino, J.J. Cooper-White, Biomaterials 35 (2014) 1150–1162.